

Experimental evidence for fast cluster formation of chain oxygen vacancies in $\text{YBa}_2\text{Cu}_3\text{O}_{7-\delta}$ being at the origin of the fishtail anomaly

Andreas Erb, Alfred A. Manuel, Marc Dhalle, Frank Marti, Jean-Yves Genoud*, Bernard Revaz, Alain Junod, Dharmavaram Vasumathi, Shoji Ishibashi†, Abhay Shukla‡, Eric Walker, Øystein Fischer and René Flükiger

Département de Physique de la Matière Condensée, Université de Genève, 24, quai Ernest Ansermet, CH-1211 Genève 4, Switzerland

Riccardo Pozzi, Mihael Mali and Detlef Brinkmann

University of Zürich, Physics Department, Winterthurerstr. 190, CH-8057 Zürich Switzerland

(Version 1.3, June 16, 2021)

Abstract

We report on three different and complementary measurements, namely magnetisation measurements positron annihilation spectroscopy and NMR measurements, which give evidence that the formation of oxygen vacancy clusters is on the origin of the fishtail anomaly in $\text{YBa}_2\text{Cu}_3\text{O}_{7-\delta}$. While in the case of $\text{YBa}_2\text{Cu}_3\text{O}_{7.0}$ the anomaly is intrinsically absent, it can be suppressed in the optimally doped state where vacancies are present. We therefore conclude that the single vacancies or point defects can not be responsible for this anomaly but that clusters of oxygen vacancies are on its origin.

PACS numbers: 74.60.G 74.60.J 74.80 74.72 76.60 78.70.B

Soon after the discovery to the 90 K superconductor $\text{YBa}_2\text{Cu}_3\text{O}_{7-\delta}$ an anomaly in the curves of the irreversible magnetisation, often referred to as *fishtail effect*, was reported [1]. This anomaly consists of an increase in the magnetisation upon increasing magnetic field which is equivalent to an increase of the critical current high above $H_{\text{c}1}$. Whereas a technical use of all other high temperature superconductors at liquid nitrogen temperatures is actually limited due to their poor critical current density in magnetic fields, the fishtail anomaly of the 123 superconductors makes them potentially useful in technical applications even at high fields. The origin of this anomaly, however, was controversially discussed for nearly a decade. Recently, we reported how the fishtail anomaly can be reversibly suppressed in the optimally doped state of $\text{YBa}_2\text{Cu}_3\text{O}_{6.92}$ and showed that it is completely absent in the fully oxygenated state $\text{YBa}_2\text{Cu}_3\text{O}_7$ [2]. In the present study, we give independent proofs for the formation of oxygen vacancy clusters being responsible for the effect. Understanding the formation mechanism of such clusters allows us to tune the pinning properties of $\text{YBa}_2\text{Cu}_3\text{O}_{7-\delta}$ to either low pinning for fundamental studies such as the investigation of vortex matter or to strong pinning by deliberately clustering the vacancies to a desired size, thus changing the critical current density and the irreversibility field.

The experiments were performed on crystals which were grown in the recently developed non-reactive crucible material BaZrO_3 [3]. Crystals obtained from such experiments exhibit a superior purity since they are not contaminated with metallic impurities from the container material [4]. Wet chemical analysis (ICP-MS) on three of the $\text{YBa}_2\text{Cu}_3\text{O}_{7-\delta}$ crystals showed that Zr, Sr and La with concentrations between 0.0005 (detection limit) and 0.001 at. %, are the only impurities. The crystals used for the oxygenation experiments exhibited the usual twinning within the a-b plane and no attempts were made to detwin the crystals. The standard annealing to obtain high transition temperatures well above 90 K in $\text{YBa}_2\text{Cu}_3\text{O}_{7-\delta}$ single crystals, consists of a treatment under 1 bar of oxygen at around 500 °C for 100 - 200 hours, followed by a quench to room temperature. However, the oxygenation of $\text{YBa}_2\text{Cu}_3\text{O}_{7-\delta}$ is performed in this way only due to the simplicity of the procedure. According to the phase diagram of Lindemer et al. [5] which gives the equilibrium oxygen concentrations

as a function of oxygen partial pressure and temperature, the same oxygen content can be obtained as well by annealing at higher temperatures in higher pressure oxygen atmospheres. The advantage of annealing at higher temperatures and higher oxygen partial pressures is that it results in an oxygenation which is presumably more homogenous and in shorter annealing times. We performed high pressure oxygen treatments at 650 - 750 °C in 100 bar of O₂ for periods of 12 - 40 h, followed by rapid quenching (about 1 min) to room temperature, so that the high temperature oxygen state can be maintained. For the case of optimally doped YBa₂Cu₃O_{7- δ} we have chosen combinations of oxygen partial pressures and temperatures which lead to the same equilibrium oxygen content in the crystal.

The magnetisation measurements were performed in a SQUID Magnetometer (Quantum Design) with the magnetic field parallel to the c-axis of the crystal. The result of an oxygenation treatment at 700 °C for 12.5 h at 100 bar can be seen in Fig. 1, where M(H) is shown for a temperature of 70 K.

No fishtail behaviour is present after this oxygenation treatment. Re-annealing the same crystal similar to the standard oxygenation (510 °C, under 1 bar oxygen) leads to the re-appearance of the fishtail anomaly, and this already after a short re-annealing time of only half an hour. If the crystal is further annealed at this temperature, the maximum in the reversible magnetisation, which was initially been re-established at a value of around 3.3 T, shifts to lower field values of about 1.5 T for an annealing time of 160 hours, whilst the amplitude of the maximum increases indicating a increase in the critical current. Note that, according to [5], the overall oxygen content of the sample has the same value of 6.92 for the three treatments and that the transition temperatures are not changed.

This time evolution of the anomaly is a direct confirmation of our earlier interpretation [2,4] of clusters of oxygen vacancies being responsible for the fishtail effect. At temperatures as high as 700 °C the oxygen deficient regions are more likely to be randomly distributed, while at lower temperatures oxygen deficient unit cells tend to cluster due to the smaller contribution of the entropy term to the free energy [2,4,6, and references therein]. Thus, when we re-anneal the crystals clusters form. Their size and mean distance however depend

on the re-annealing time. Short time annealing produces small and densely spaced clusters, which grow, when annealing progresses, to bigger size with larger distances. Pinning of vortices is most effective if the distance between vortices matches to the mean distance between the pinning centers. In the case of pinning by oxygen vacancy clusters, we find, for the short re-annealing time of half an hour a maximum for the critical current at higher fields (3.3 Tesla), which is shifted to lower fields for longer annealing times, when cluster growth makes their mean distance larger. On the other hand the amplitude of the maximum increases for the longer anneals since the bigger clusters have a higher pinning potential.

A simple picture defining the maximum of the anomaly as a matching field enables us to calculate the average spacing between oxygen vacancy clusters. Doing so we find a spacing of about 25 nm for a matching field of 3.3 T and 37 nm for the maximum at 1.5 T respectively. Assuming that all vacancies present within the space between clusters would contribute to its formation and that the clusters consist of $\text{YBa}_2\text{Cu}_3\text{O}_{6.0}$, one calculates for the present concentration of $\text{YBa}_2\text{Cu}_3\text{O}_{6.92}$ that around 350 vacancies are in a clustered state after the short term annealing. Thus an upper limit for the size of a cluster is about 18 x18 unit cells. For longer annealing these clusters would then contain some 750 vacancies, setting the upper limit for cluster sizes to 27 x 27 unit cells. We note here that certainly not all vacancies are in a clustered state since T_c remains unchanged, so that the estimation above only gives an upper limit for the size.

That such a short range reorganisation of the vacancies is indeed possible can be seen by calculating the effective diffusion length, using the diffusion coefficients measured on identical samples [7,8]. The chemical diffusion coefficient, which is the product of the self-diffusion coefficient and the thermodynamic factor, turned out to be $8 \times 10^{-8} \text{ cm}^2/\text{s}$ at 510 °C with the thermodynamic factor being about 10 [9,10]. Using the Einstein formula $d_{eff} = \sqrt{6D_{self}(T)t}$, an estimation of the effective diffusion length for the short re-annealing of half an hour yields a possible migration of vacancies of about 90 mm, which is far more than needed.

Among the methods, which allow us to study the oxygen vacancies more directly, are the positron annihilation technique and NMR which we will discuss now. Both methods probe

bulk properties and this on a microscopic level. In addition, these techniques do not alter the oxygen vacancy distribution.

Positron annihilation spectroscopy [11] is site-sensitive and probes bulk properties. Measured spectra depend strongly on the chemical and structural environment of the annihilating positron. In $\text{YBa}_2\text{Cu}_3\text{O}_{7-\delta}$, it has been established that the positrons i) annihilate in the region of the copper-oxygen chains [12]; ii) tend to localize near oxygen vacancies which function as weak *traps* [13]; and iii) are trapped more efficiently by larger oxygen vacancy clusters [14].

We have measured the quantity $N(p_x, p_y)$, the electron momentum density sampled by the annihilating positrons. The temperature of the twinned $\text{YBa}_2\text{Cu}_3\text{O}_{7-\delta}$ single crystal was 177 °C to favour the thermally activated migration of the positrons trapped by shallow structural defects like single oxygen vacancies [13]. The momentum-dependent annihilation lines $N(p_x, 0)$ are shown in Fig. 2 for the three different sample treatments: a) fully oxygenated (triangles), b) optimally doped without fishtail (squares) and c) optimally doped with fishtail (circles). The $N(p_x, p_y)$ distributions were normalised to equal area. The peak height of $N(p_x, 0)$, in a sample containing defects acting as positron traps, corresponds to the degree of positron localization. Trapped positrons are more likely to annihilate with valence electrons than with bound core electrons of higher momenta (see [11]), giving rise to a line more peaked at the zero momentum. We observe the lowest peak (indicating delocalized positrons) in the case of the fully oxygenated $\text{YBa}_2\text{Cu}_3\text{O}_{7-\delta}$, as there is no trapping by oxygen vacancies. In the optimally doped state with fishtail, the annihilation line has the highest peak. This signifies the presence of large clusters of oxygen vacancies which act as more efficient positron traps than single oxygen vacancies or small clusters [13]. In the optimally doped state without fishtail, the peak height is somewhat larger than for the fully oxygenated state, indicating weak positron trapping, which is attributed to residual trapping by clusters too small to act as pinning centres for vortices. Our interpretation is further confirmed by the difference of peak height previously observed between $\text{YBa}_2\text{Cu}_3\text{O}_6$ (insulating) and $\text{YBa}_2\text{Cu}_3\text{O}_7$ crystals [15]. $\text{YBa}_2\text{Cu}_3\text{O}_6$ shows the highest peak height, sim-

ilar to what we observe for the optimally doped state with fishtail. This is in agreement with the fact that, in a large oxygen vacancy cluster, the positron sees a local environment corresponding to the $\text{YBa}_2\text{Cu}_3\text{O}_6$ phase.

The correlation between the large peak height in $N(p_x, 0)$ and the presence of the fishtail leads us to conclude that the fishtail anomaly in the magnetisation is a peak effect induced by the clustering of the oxygen vacancies.

Finally, we will discuss our NMR studies which probe microscopically the arrangement of the oxygen vacancies. We employed Cu NMR which is an appropriate method since the resonance frequency of Cu1 (chain copper) depends strongly on the co-ordination by nearest-neighbour oxygen ions. The magnetic shift and the electric field gradient tensors are well-known for plane copper, Cu2 [16], copper in a filled chain, $(\text{Cu1})_4$, i.e. co-ordinated by four oxygen ions [16] and copper in an empty chain, $(\text{Cu1})_2$, i.e. co-ordinated by two apex oxygen only [17]. We investigated a single crystal whose magnetization curves, for two oxygenation states, are shown in Fig. 3. For the $\text{YBa}_2\text{Cu}_3\text{O}_7$ state, NMR yielded four Cu peaks (Fig. 4a): Two of them are very narrow and correspond to the Cu2 and $(\text{Cu1})_4$ central lines ($-1/2 \leftrightarrow +1/2$ transitions) of the quadrupolar splitting and the broader double peak at 102.15 MHz consists of the two satellite lines ($\pm 3/2 \leftrightarrow \pm 1/2$ transitions) of $(\text{Cu1})_4$. The intensity of a line is given by the integral over the line and is proportional to the number of nuclear spins contributing to the corresponding line. As expected by virtue of the crystal structure, the intensity of the Cu2 central line turned out to be roughly twice the intensity of the $(\text{Cu1})_4$ central line. The absence of other Cu lines indicates that the chains are perfectly filled and thus confirms the extremely low defect concentration of the fully oxygenated crystal. In addition, a tiny signal of sodium showed up at 101.3 MHz, probably stemming from sweat in the crumpled piece of cotton wool fixing the crystal.

Next, we investigated the $\text{YBa}_2\text{Cu}_3\text{O}_{6.9}$ state. If the crystal is annealed at 510 °C, the lines discussed above become much broader (Fig. 4b). Furthermore, a new signal appears at 101.4 MHz that corresponds to chain $(\text{Cu1})_2$. By comparing the Cu2 and $(\text{Cu1})_2$ line intensities, corrected for their spin-spin relaxation times and frequencies, we conclude

that 5 - 10% of all chain Cu ions are co-ordinated by an oxygen vacancy on either side. Furthermore, the very narrow $(\text{Cu1})_2$ line (with a "full width half height" of 13 kHz) reveals a high degree of local order at this site, indicating that $(\text{Cu1})_2$ must be located in rather large empty-chain clusters. The formation of such large clusters would also explain why we did not detect $(\text{Cu1})_3$ signals which would arise from Cu sites with only one oxygen vacancy neighbour in the chain. The $(\text{Cu1})_3$ site appears at the interface between filled and empty chain segments with a relative abundance that diminishes with increasing length of the empty segments. The corresponding NMR experiments with $\text{YBa}_2\text{Cu}_3\text{O}_{6.9}$ and suppressed fishtail are in progress. However, they are very time consuming since the sample size must be kept sufficiently small to allow a high quenching rate which is necessary for a complete suppression of the anomaly.

In conclusion three different and complementary measurements give evidence that the formation of oxygen vacancy clusters is the origin of the fishtail anomaly in $\text{YBa}_2\text{Cu}_3\text{O}_{7-\delta}$. Note, that the single vacancies or point defects can not be responsible for this anomaly, since this anomaly can also be suppressed in the optimally doped state where vacancies are present. Thus, a formation mechanism that leads to larger nevertheless still microstructural inhomogeneities must be responsible for this effect. In the case of $\text{YBa}_2\text{Cu}_3\text{O}_{7.0}$ the anomaly is intrinsically absent unless the crystals contain metallic impurities. On such $\text{YBa}_2\text{Cu}_3\text{O}_{7.0}$ samples melting of the vortex lattice has been observed by calorimetric measurements [18] as a first order transition between 4 and 26.5 T, which was the highest available field, giving further support for our interpretation and yields new insight into the nature of vortex matter. For application purposes the understanding of the formation mechanism of microstructural inhomogeneities offers the possibility to tailor the samples according to the required properties influencing the maximum value of the critical current and the irreversibility field.

REFERENCES

* Present address: Industrial Research Limited, PO Box 31-310, Lower Hutt, New Zealand.

† Permanent address: Electrotechnical Laboratory, Tsukuba, Ibaraki 305-8568, Japan.

‡ Permanent address: High Energy Group, ESRF, BP 220, F-38043 Grenoble, France.

- [1] M. Däumling, J. M. Seuntjens, D. C. Larbalestier, *Nature* **346**, 332 (1990).
- [2] A. Erb, J.-Y. Genoud et al., *J. of Low Temp. Phys.* **105**, 1023 (1996).
- [3] A. Erb, E. Walker, R. Flükiger, *Physica C* **245**, 245 (1995); A. Erb, E. Walker, R. Flükiger, *Physica C* **258**, 9 (1996).
- [4] A. Erb, E. Walker, J.-Y. Genoud, R. Flükiger, *Physica C* 282-287, **89** (1997).
- [5] T. B. Lindemer et al., *J. Am. Ceram. Soc.*, **72**, 1775 (1989).
- [6] J. L. Vargas and D. C. Larbalestier, *Appl. Phys. Lett.* **60**, 1741 (1992).
- [7] A. Erb, B. Greb and G. Müller-Vogt, *Physica C* **259**, 83 (1996).
- [8] M. Kläser, J. Kaiser, F. Stock and G. Müller-Vogt, A. Erb, submitted to *Physica C*.
- [9] K. Conder and Ch. Krüger, *Physica C* **269**, 92 (1996).
- [10] F. Faupel et al. *Z. Metallkd.* **84**, 8 (1993).
- [11] A. Dupasquier and A.P. Mills jr, ed., *Positron Spectroscopy of Solids* (OPS Press, Amsterdam, 1995).
- [12] E.C. von Stetten, S. Berko, X.S. Li, R.R. Lee, J. Brynestad, D. Singh, H. Krakauer, W.E. Pickett and R.E. Cohen, *Phys. Rev. Lett.* **60**, 2198 (1988).
- [13] M. Peter, A. Shukla, L. Hoffmann and A.A. Manuel, *Nuova Acta Leopoldina NF* **72**, Nr. 294, p. 257 (1996); A. Shukla, PhD thesis Nr. 2744, University of Geneva, (1995).

- [14] S. Ishibashi, R. Yamamoto, M. Doyama and T. Matsumoto, *J. Phys. Condens. Matter* **3**, 9169 (1991).
- [15] B. Barbiellini, P. Genoud, J.Y. Henry, L. Hoffmann, T. Jarlborg, A.A. Manuel, S. Massidda, M. Peter, W. Sadowski, H.J. Scheel, A. Shukla, A.K. Singh and E. Walker, *Phys. Rev. B* **43**, 7810 (1991).
- [16] C. H. Pennington, D. J. Durand, C. P. Slichter, J. P. Rice, E. D. Bukowski, and D. M. Ginsberg, *Phys. Rev. B* **39**, 2902 (1989).
- [17] M. Mali, I. Mangelschots, H. Zimmermann, and D. Brinkmann, *Physica C* **175**, 581 (1991).
- [18] A. Junod et al. *Physica C* **275**, 245 (1997); M. Roulin et al. *Phys. Rev. Lett.* **80**, 1722 (1998); F. Bouquet and C. Marcenat, private communication.

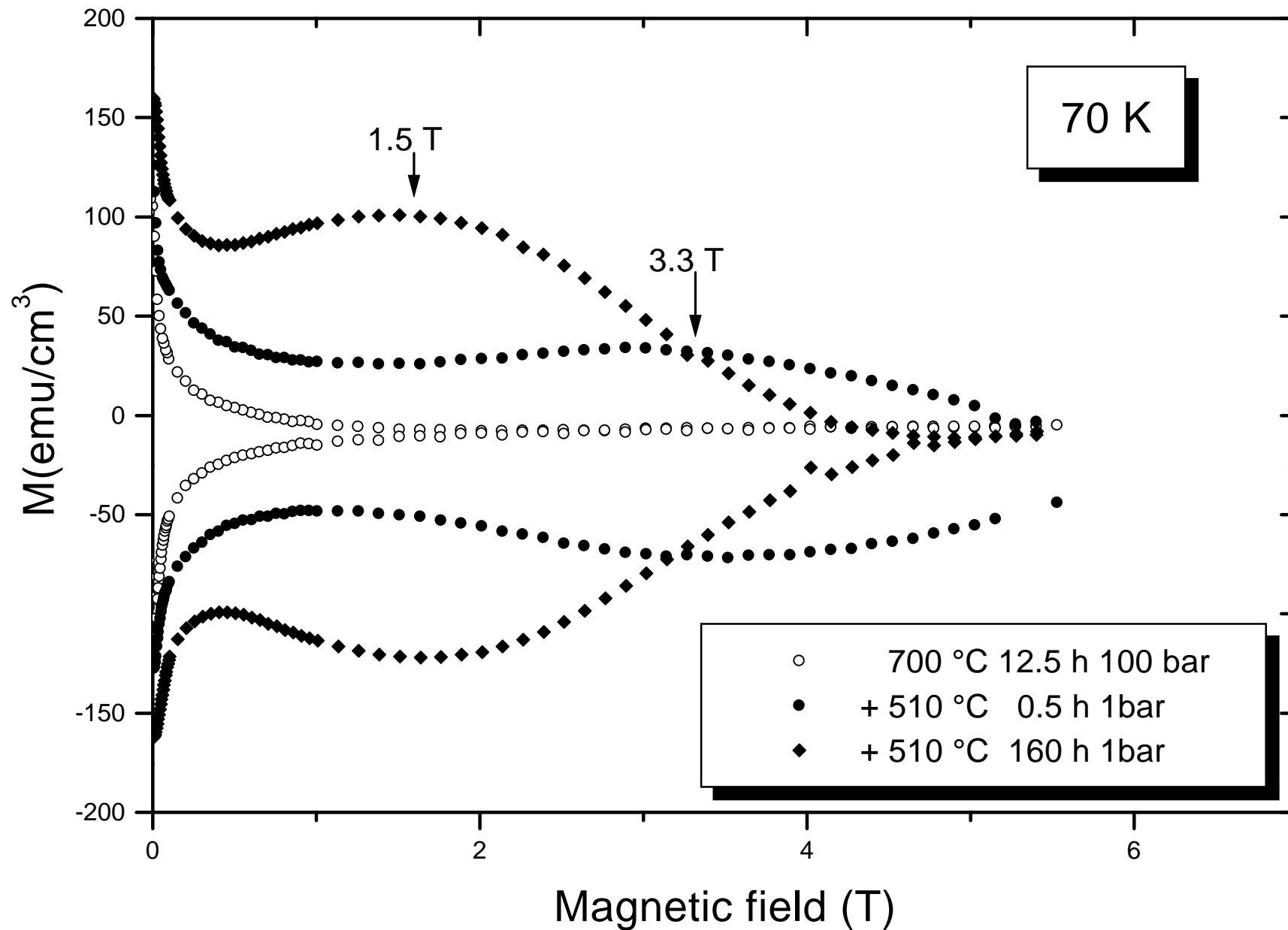
FIGURES

FIG. 1. Magnetisation of $\text{YBa}_2\text{Cu}_3\text{O}_{6.92}$ at 70 K after different annealing regimes. The fishtail anomaly is re-established already after short annealing times and moves to lower field values for longer anneals.

FIG. 2. Momentum-dependent positron annihilation lines for $\text{YBa}_2\text{Cu}_3\text{O}_{6.9}$ with fishtail (circles), without fishtail (squares) and for $\text{YBa}_2\text{Cu}_3\text{O}_7$ (triangles).

FIG. 3. Magnetisation curves at 70 K of $\text{YBa}_2\text{Cu}_3\text{O}_x$ - single crystal AE276G after full oxygenation to a O_7 (empty symbols) and $\text{O}_{6.90}$ (full symbols).

FIG. 4. ^{63}Cu central (and satellite) lines of different sites are shown (a) for $\text{YBa}_2\text{Cu}_3\text{O}_7$ and (b) for $\text{YBa}_2\text{Cu}_3\text{O}_{6.9}$ at room temperature. The external magnetic field (8.995 Tesla) was oriented along the c-axis of the single crystal. The indicated linewidths are defined as the full widths at half maximum. The insets show the full size of the lines.



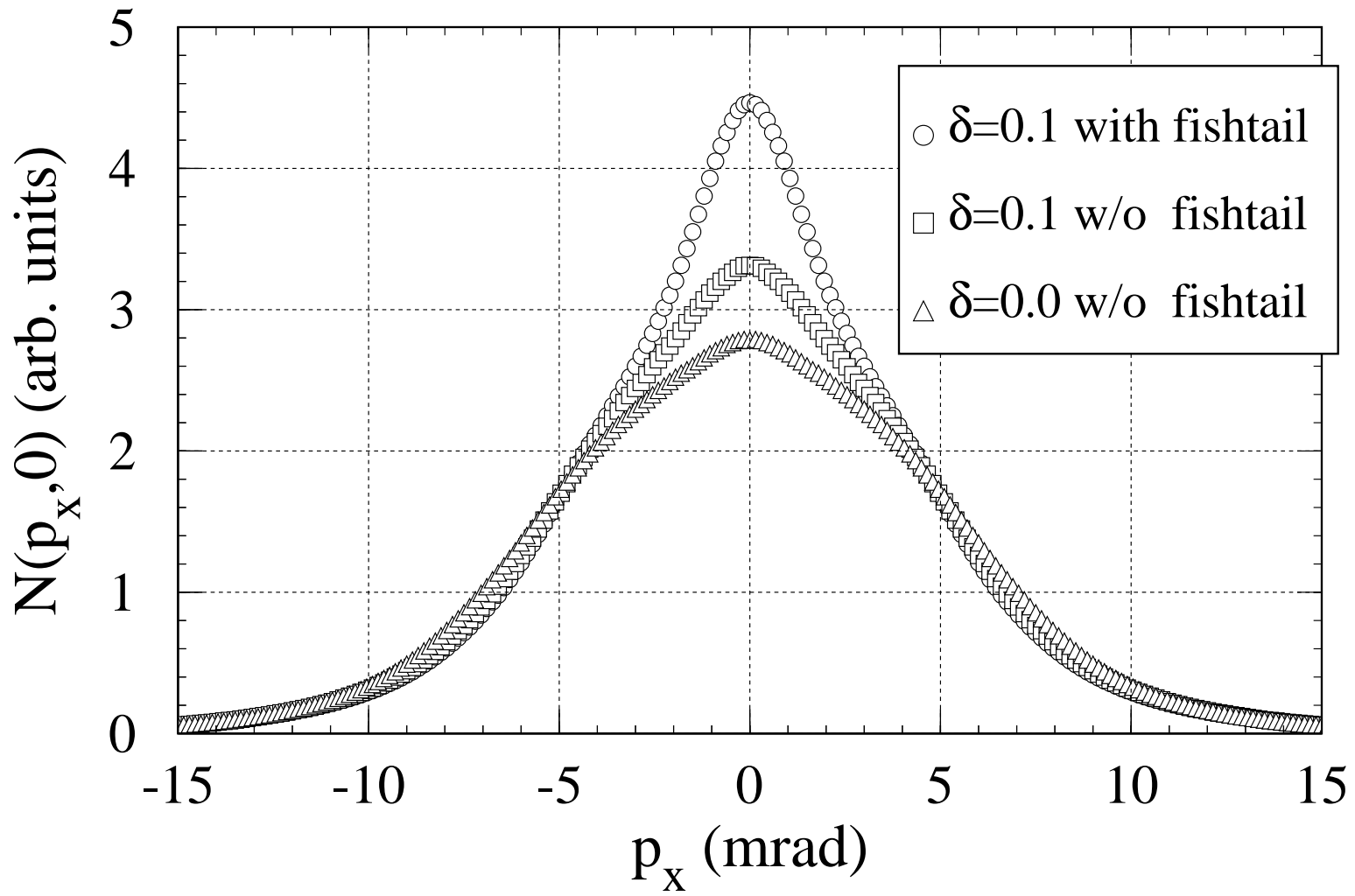


Figure 2. Erb et al.)

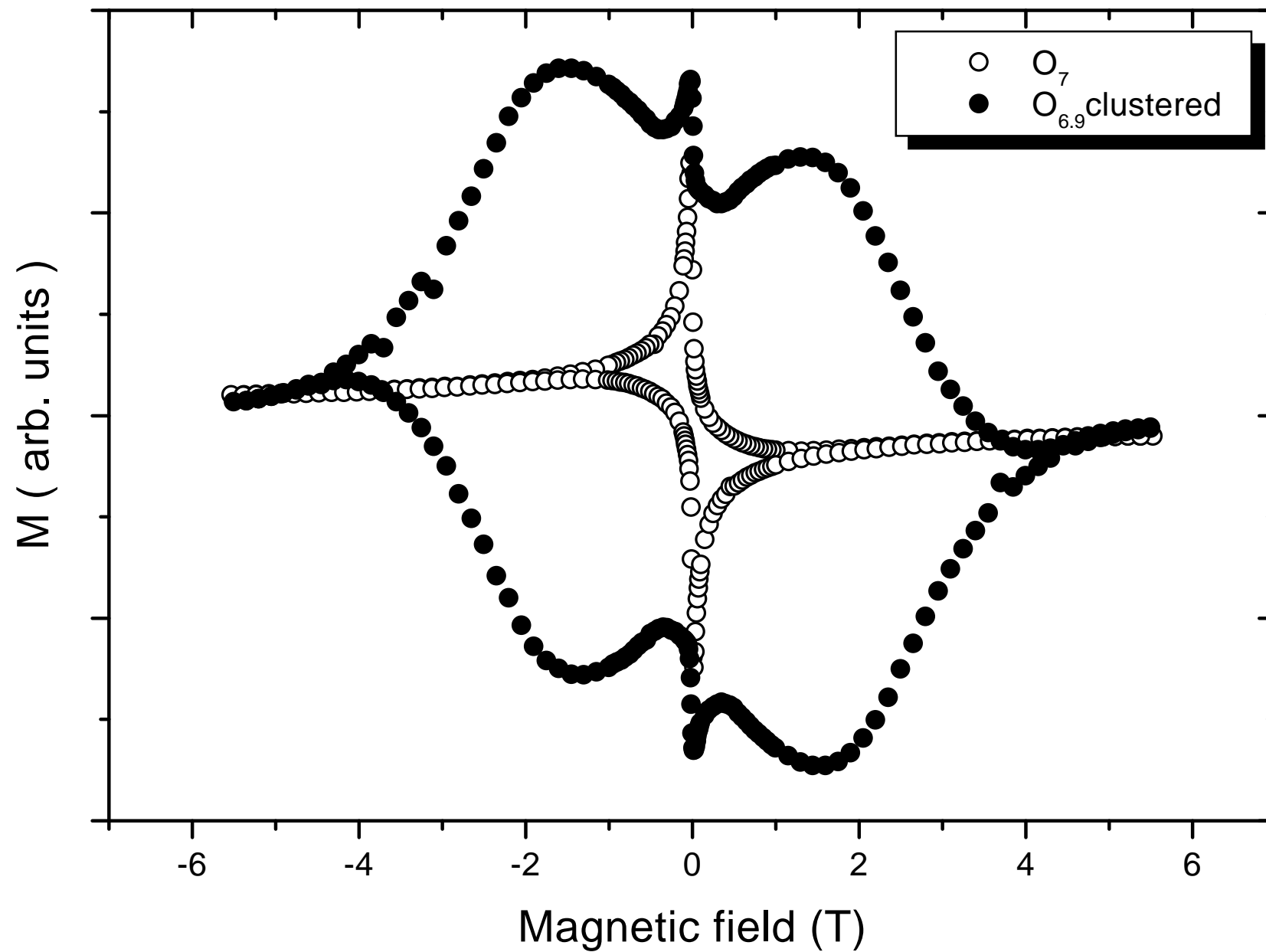


Figure 4

